

Dispersive analysis of $K_{L\mu 3}$ and $K_{Le 3}$ scalar and vector form factors using KTeV data

E. Abouzaid,⁴ M. Arenton,¹¹ A.R. Barker,^{5,*} L. Bellantoni,⁷ E. Blucher,⁴ G.J. Bock,⁷ E. Cheu,¹ R. Coleman,⁷ M.D. Corcoran,⁹ B. Cox,¹¹ A.R. Erwin,¹² C.O. Escobar,³ A. Glazov,⁴ R.A. Gomes,³ P. Gouffon,¹⁰ Y.B. Hsiung,⁷ D.A. Jensen,⁷ R. Kessler,⁴ K. Kotera,⁸ A. Ledovskoy,¹¹ P.L. McBride,⁷ E. Monnier,^{4,†} H. Nguyen,⁷ R. Niclasen,⁵ D.G. Phillips II,¹¹ E.J. Ramberg,⁷ R.E. Ray,⁷ M. Ronquest,¹¹ E. Santos,¹⁰ W. Slater,² D. Smith,¹¹ N. Solomey,⁴ E.C. Swallow,^{4,6} P.A. Toale,⁵ R. Tschirhart,⁷ Y.W. Wah,⁴ J. Wang,¹ H.B. White,⁷ J. Whitmore,⁷ M. J. Wilking,⁵ R. Winston,⁴ E.T. Worcester,⁴ T. Yamanaka,⁸ E. D. Zimmerman,⁵ and R.F. Zukanovich¹⁰

(KTeV Collaboration)

Véronique Bernard,^{13,‡} Micaela Oertel,^{14,§} Emilie Passemar,^{15,¶} and Jan Stern^{13,**}

¹University of Arizona, Tucson, Arizona 85721

²University of California at Los Angeles, Los Angeles, California 90095

³Universidade Estadual de Campinas, Campinas, Brazil 13083-970

⁴The Enrico Fermi Institute, The University of Chicago, Chicago, Illinois 60637

⁵University of Colorado, Boulder, Colorado 80309

⁶Elmhurst College, Elmhurst, Illinois 60126

⁷Fermi National Accelerator Laboratory, Batavia, Illinois 60510

⁸Osaka University, Toyonaka, Osaka 560-0043 Japan

⁹Rice University, Houston, Texas 77005

¹⁰Universidade de São Paulo, São Paulo, Brazil 05315-970

¹¹The Department of Physics and Institute of Nuclear and Particle Physics, University of Virginia, Charlottesville, Virginia 22901

¹²University of Wisconsin, Madison, Wisconsin 53706

¹³Groupe de Physique Théorique, IPN, Université de Paris Sud-XI, F-91406 Orsay, France

¹⁴LUTH, Observatoire de Paris, CNRS, Université Paris Diderot, 5 place Jules Janssen, 92195 Meudon, France

¹⁵Albert Einstein Center for Fundamental Physics, Institute for theoretical physics, University of Bern, Sidlerstr. 5, CH-3012 Bern, Switzerland

Using the published KTeV samples of $K_L \rightarrow \pi^\pm e^\mp \nu$ and $K_L \rightarrow \pi^\pm \mu^\mp \nu$ decays [1], we perform a reanalysis of the scalar and vector form factors based on the dispersive parameterization [2, 3]. We obtain phase space integrals $I_K^e = 0.15446 \pm 0.00025$ and $I_K^\mu = 0.10219 \pm 0.00025$. For the scalar form factor parameterization, the only free parameter is the normalized form factor value at the Callan-Treiman point (C); our best fit results in $\ln C = 0.1915 \pm 0.0122$. We also study the sensitivity of C to different parametrizations of the vector form factor. The results for the phase space integrals and C are then used to make tests of the Standard Model. Finally, we compare our results with lattice QCD calculations of F_K/F_π and $f_+(0)$.

PACS numbers: 13.25.Es, 11.55.Fv

I. INTRODUCTION

Recently, much effort has been devoted to measure the vector and scalar $K\pi$ form factors in semileptonic kaon decays in order to determine the phase space integrals. These integrals, along with the kaon branching fractions, allow to determine the CKM matrix element $|V_{us}|$. The scalar form factor (f_0) is difficult to measure because it is kinematically suppressed in K_{e3} decays, and is therefore

only measurable in $K_{\mu 3}$ decays, which have contributions from both the scalar and vector form factors. In addition, with the present experimental precision, only one f_0 model parameter can be accurately measured (see e.g. [4]). Until recently, these form factors were determined with Taylor and pole parametrizations [1, 5, 6, 7]:

$$\begin{aligned} \bar{f}_{+,0}^{Tayl}(t) &= 1 + \lambda'_{+,0} \frac{t}{M_\pi^2} + \frac{1}{2} \lambda''_{+,0} \left(\frac{t}{M_\pi^2} \right)^2 \\ &\quad + \frac{1}{6} \lambda'''_{+,0} \left(\frac{t}{M_\pi^2} \right)^3 + \dots \end{aligned} \quad (1)$$

$$\bar{f}_{+,0}^{Pole}(t) = \frac{M_{V,S}^2}{M_{V,S}^2 - t}, \quad (2)$$

where $t = (p_K - p_\pi)^2$ is the expansion parameter as a function of the kaon and pion four-momenta, and $\bar{f}_{+,0}(t) \equiv f_{+,0}(t)/f_{+,0}(0)$ are the normalized vector and

*Deceased.

†Permanent address C.P.P. Marseille/C.N.R.S., France

‡Email: bernard@ipno.in2p3.fr

§Email: micaela.oertel@obspm.fr

¶Email: passemar@itp.unibe.ch. Present address: IFIC, Universitat de València - CSIC, Apt. Correus 22085, E-46071 València, Spain

**Jan Stern sadly passed away before this paper was completed.

scalar form factors. The parameters measured in a fit to the data are $\lambda'_{+,0}$ and λ'_+ , the slope of the form factors and the curvature of the vector one, and $M_{V,S}$, the mass of the vector and scalar resonances. While the second order Taylor expansion has been used to measure the vector form factor with sufficient precision, the scalar form factor can only be determined using the first-order Taylor expansion or the pole model. However, clearly one has at least to know the curvature to have a proper description of $f_0(t)$ in the physical region of $K_{\ell 3}$ -decays. After results were reported based on the Taylor and pole parametrizations, a form factor parametrization based on conformal mapping was discussed in Ref. [8] in the context of $B \rightarrow \pi l \nu$ to improve the convergence of the series and to give rigorous bounds on its coefficients. This parametrization was applied to the $K_{\ell 3}$ case in Ref. [9], and recently used by the KTeV collaboration to reanalyze their K_{e3} data [10].

As an alternative approach, the dispersive parametrization in Refs. [2, 3] has the advantage to account for the correlation between the slope and the curvature, by using low energy $K\pi$ phase shifts [11, 12, 13]. It involves only one free parameter for both the scalar and vector form factors to be determined from the existing data sample. The sole scalar form factor parameter is C , the value of the normalized scalar form factor at the Callan-Treiman (CT) point, $t \equiv \Delta_{K\pi} = m_K^2 - m_\pi^2$, the difference of kaon and pion masses squared. Once C is determined, the shape of the scalar form factor is known with a high precision in the physical region and somewhat beyond. The choice of this particular parameter C is guided by the existence of the Callan-Treiman theorem [14] which predicts its value in the $SU(2) \times SU(2)$ chiral limit. For physical quark masses,

$$C \equiv \bar{f}_0(\Delta_{K\pi}) = \frac{F_{K^+}}{F_{\pi^+}} \frac{1}{f_+^{K^0\pi^-}(0)} + \Delta_{CT} . \quad (3)$$

where F_π and F_K are the pion and kaon decay constants, respectively, and Δ_{CT} is a correction of order $\mathcal{O}(m_{u,d}/4\pi F_\pi)$ arising from non zero quark masses m_u, m_d . This correction has been evaluated within Chiral Perturbation Theory (ChPT) and is small enough that the right-hand side of Eq. (3) can be determined with sufficient accuracy as discussed in § IV to compare with C measured in $K_{\mu 3}$ -decays. Thus apart from the determination of $|V_{us}|$, which is used to test the unitarity of the CKM matrix within the Standard Model (SM), a measurement of the scalar form factor at the Callan Treiman point provides another interesting test of the SM, namely a test of the couplings of light quarks to W . Another interest in the experimental determination of the shape of the $K\pi$ scalar form factor is the possibility of determining low energy constants which appear in ChPT [29].

The NA48 [15] and KLOE [16] collaborations have re-analyzed their data with the dispersive parameterization [2]. The values of C obtained in these two experiments

differ by 2.1σ . Here we present a similar reanalysis of the KTeV data [1] leading to an improvement on the precision on the determination of the form factors compared with the previous KTeV results [1, 10]. Since the vector and scalar form factors are correlated, alternative parametrizations for the vector form factor are studied to probe the robustness of the scalar form factor result.

The paper is organized as follows. In § II we present the results of the dispersive analysis of the KTeV data. In § III we discuss the correlations between the vector and the scalar form factor. § IV is devoted to a discussion of different applications of our results, in particular the test of the SM. We summarize in § V.

II. DISPERSIVE ANALYSIS OF KTeV SEMILEPTONIC DATA

Assuming $\bar{f}_0(t)$ is never equal to zero, the dispersive representation for the normalized scalar form factor reads

$$\bar{f}_0(t) = \exp\left[\frac{t}{\Delta_{K\pi}}(\ln C - G(t))\right], \quad (4)$$

$$G(t) = \frac{\Delta_{K\pi}(\Delta_{K\pi} - t)}{\pi} \times \int_{(m_K+m_\pi)^2}^{\infty} \frac{ds}{s} \frac{\phi_0(s)}{(s - \Delta_{K\pi})(s - t - i\epsilon)}. \quad (5)$$

Note that C is here the only free parameter. $\phi_0(s)$ represents the phase of the form factor: following Watson's theorem [17], this phase is equal to the $K\pi$ scattering phase within the elastic region. In writing Eq. (4), two subtractions have been made to minimize the unknown high energy contribution to the dispersive integral, Eq. (5). The two subtraction points have been taken at $t = 0$ and at the CT point to take advantage of the CT theorem, Eq. (3). The resulting function $G(t)$ in Eq. (5) does not exceed 20% of the expected value of $\ln C$; since theoretical uncertainties on $G(t)$ are $\sim 10\%$ its value, the corresponding uncertainty on $\ln C$ is then a few percent of its value.

The dispersive representation of the vector form factor is constructed in a similar manner. Since there is no analog of the CT theorem in this case, the two subtractions are performed at $t = 0$. The normalized vector form factor is

$$\bar{f}_+(t) = \exp\left[\frac{t}{m_\pi^2}(\Lambda_+ + H(t))\right], \quad (6)$$

$$H(t) = \frac{m_\pi^2 t}{\pi} \int_{(m_K+m_\pi)^2}^{\infty} \frac{ds}{s^2} \frac{\phi_+(s)}{(s - t - i\epsilon)}, \quad (7)$$

where $\Lambda_+ \equiv m_\pi^2 d\bar{f}_+(t)/dt|_{t=0}$ and $\phi_+(s)$ is the phase of the vector form factor. As in the case for the scalar form factor, information on the $K\pi$ phase shifts in the elastic region is used to determine $\phi_+(s)$. The main contribution to $\phi_+(s)$ is the dominant $K^*(892)$ resonance. The extrapolation of the $K\pi$ phase shift data down to

	K_{e3} only	$K_{\mu3}$ only	K_{e3} and $K_{\mu3}$ Combined
$\Lambda_+ \times 10^3$	25.17 ± 0.62	24.57 ± 1.10	25.09 ± 0.55
$\ln C$	-	0.1947 ± 0.0140	0.1915 ± 0.0122
$\rho(\Lambda_+, \ln C)$	-	-0.557	-0.269
χ^2/dof	66.6/65	193/236	0.48/2
$\lambda'_+ \times 10^3$	25.17 ± 0.62	24.57 ± 1.10	25.09 ± 0.55
$\lambda''_+ \times 10^3$	1.22 ± 0.07	1.19 ± 0.07	1.21 ± 0.08
$\lambda_0 \times 10^3$	-	13.22 ± 1.39	12.95 ± 1.17
$\lambda'_0 \times 10^3$	-	0.59 ± 0.05	0.58 ± 0.05
I_K^e	0.15450 ± 0.00028	0.15416 ± 0.00060	0.15446 ± 0.00025
I_K^μ	-	0.10207 ± 0.00032	0.10219 ± 0.00025
I_K^μ/I_K^e	-	0.6621 ± 0.0018	0.6616 ± 0.0015

TABLE I: Results of the analysis of the KTeV K_{Le3} and $K_{L\mu3}$ data using a dispersive parameterization for the vector and scalar form factors. Λ_+ and $\ln C$ are the parameters of the fit used to calculate the slopes, curvatures and the phase space integrals. The uncertainties correspond to the total ones, adding the statistic, the systematic as well as the theoretical ones in quadrature, see the text for more details.

threshold is done here following a Gounaris-Sakurai construction based on the $K^*(892)$ and exhibiting the correct threshold behavior and the correct properties of analyticity and unitarity. The value of $H(t)$ represents at most 20% of the value of Λ_+ such that the latter can be measured with high precision. For more details on the dispersive representations, see Refs. [2] and [3].

In Ref. [3], a thorough discussion of the different sources of theoretical uncertainties of the dispersive representations can be found. They include the error on the low energy $K\pi$ phase shifts and an estimate of the uncertainties due to the unknown high energy behaviour of the phases $\phi_0(s)$ and $\phi_+(s)$. The corresponding error-bands, $\delta G(t)$ and $\delta H(t)$, are used in this analysis to propagate uncertainties on Λ_+ and $\ln C$.

The analysis of the KTeV data is done using their K_{Le3} and $K_{L\mu3}$ samples with 1.9×10^6 and 1.5×10^6 events, respectively after selection requirements. These samples were collected in a special run in which the beam intensity was lowered by a factor of ten compared to that used to measure ϵ'/ϵ . The laboratory-frame kaon energies are 40-160 GeV (mean is 70 GeV), and the momenta of charged particles are measured with much better than 1% precision. Muons are identified with a large scintillator hodoscope behind 3 meters of steel. Electrons and pions are identified primarily by ratio of energy deposited in the cesium iodide calorimeter (E) to the momentum measured in a magnetic spectrometer (p); $E/p \sim 1$ for electrons, and $E/p < 1$ for pions. In addition to using the KTeV data, we also use the KTeV Monte Carlo (MC) to correct for the detector acceptance that results in a non-uniform sampling of the $K_{\ell3}$ Dalitz plot.

The results of the dispersive analysis are given in Table I. The associated slope and curvature are also given, based on Taylor expansions of Eqs. (4) and (6) using the best-fit values of $\ln C$ and Λ_+ , respectively. A combined

K_{e3} and $K_{\mu3}$ dispersive analysis leads to

$$\begin{aligned}
\Lambda_+ &= 0.02509 \pm 0.00035_{\text{stat}} \pm 0.00027_{\text{sys}} \pm 0.00033_{\text{th}} \\
&= 0.02509 \pm 0.00055, \\
\ln C &= 0.1915 \pm 0.0078_{\text{stat}} \pm 0.0086_{\text{sys}} \pm 0.0038_{\text{th}} \\
&= 0.1915 \pm 0.0122.
\end{aligned} \tag{8}$$

The phase space integrals are then given by:

$$\begin{aligned}
I_K^e &= 0.15446 \pm 0.00019_{\text{stat}} \pm 0.00015_{\text{sys}} \pm 0.00008_{\text{th}} \\
&= 0.15446 \pm 0.00025, \\
I_K^\mu &= 0.10219 \pm 0.00017_{\text{stat}} \pm 0.00017_{\text{sys}} \pm 0.00005_{\text{th}} \\
&= 0.10219 \pm 0.00025.
\end{aligned} \tag{9}$$

Systematic uncertainties are estimated following the prescription of Ref. [10], by scaling the ratio of systematic-to-statistical uncertainties for the pole model in Table 1 of Ref. [1] (see Eq. (15) of Ref. [10]). Statistical, systematic and theoretical uncertainties are added in quadrature to give the total uncertainty. To estimate the theoretical error on $\ln C$ and Λ_+ induced by uncertainties on the functions $G(t)$ and $H(t)$ entering the dispersive representations, we perform fits using $G(t) \pm \delta G(t)$ and $H(t) \pm \delta H(t)$. The function $G(t)$ is positively correlated with $\ln C$, and $H(t)$ is negatively correlated with Λ_+ ; these correlations lead to reduced uncertainties in the phase-space integrals (I_K).

Table I provides also values of the phase space integrals ratio, I_K^μ/I_K^e . Note that for them the estimated total uncertainty takes into account correlation due to the common vector form factor $f_+(t)$ which reduces the uncertainty.

After subtracting the common theoretical uncertainties, our result for $\ln C$ is consistent with the KLOE result, $\ln C = 0.2038(246)$ [16], and it is 2.6σ larger than the NA48 result, $\ln C = 0.1438(140)$ [15]. For the previous form factor fits from KTeV [1], the phase-space integrals ($I_K^e = 0.15350(105)$, $I_K^\mu = 0.10165(80)$) are in good agreement with the dispersive results above, but the precision is limited by modeling uncertainties

that are twice as large as the statistical errors. The large modeling uncertainty in Ref. [1] is based on the difference between using the pole model ($I_K^e = 0.15445(23_{stat}), I_K^\mu = 0.10235(22_{stat})$) and the quadratic model ($I_K^e = 0.15350(44_{stat}), I_K^\mu = 0.10165(39_{stat})$), where the uncertainties are statistical only; the pole model result agrees very well with the result above based on the dispersive analysis. For the z -parameterization [10] ($I_K^e = 0.15392(48)$), the theoretical uncertainty is slightly larger than that from the dispersive analysis, and therefore the I_K^e -discrepancy may be significant. To investigate this difference, several Monte Carlo samples were generated using input form factors from the result of the dispersive fit and subsequently analysed using z -parameterization. Based on this study, the I_K integrals obtained with the z -parameterization reproduce on average the input value, and the difference between the z and dispersive parameterization observed for the KTeV data is consistent with a $1.8\sigma_{stat}$ fluctuation.

III. COMPARISON OF DIFFERENT FORM FACTOR PARAMETERIZATIONS

As pointed out in the introduction, a main advantage of the dispersive parameterization is the possibility of determining the value of the scalar form factor at the Callan-Treiman point, thus allowing for a test of the SM. At present, only the dispersive parameterization makes it possible to determine the scalar form factor at this point, which lies far beyond the endpoint of the physical region, with reasonable precision. Since there is a large correlation between $\ln C$ and the slope of the vector form factor (see $\rho(\Lambda_+, \ln C)$ in Table I), however, it is important to study the sensitivity of $\ln C$ to the choice of parameterization for the vector form factor.

To investigate this sensitivity, we have fit the KTeV data using the dispersive parameterization for the scalar form factor (with $\ln C$ as a free parameter) and four different parameterizations for the vector form factor:

- the dispersive parameterization Eq. (6)
- the pole parameterization Eq. (2)
- the quadratic (second-order) Taylor expansion Eq. (1)
- the z -parameterization

$$F_+(t) = F_+(t_0) \frac{\phi_+(t_0, t_0, Q^2)}{\phi_+(t, t_0, Q^2)} \sum_{k=0}^{\infty} a_k(t_0, Q^2) z(t, t_0)^k, \quad (10)$$

$$\bar{f}_+(t) = F_+(t)/F_+(0),$$

based on a conformal mapping of t onto the variable z with

$$z(t, t_0) \equiv \frac{\sqrt{t_+ - t} - \sqrt{t_+ - t_0}}{\sqrt{t_+ - t} + \sqrt{t_+ - t_0}}. \quad (11)$$

In Eq. (10) we have used the notation from Ref. [9].

The results of these fits are summarized in Tables II and III. The “dispersive” results are taken from Section II. All of the fits have good χ^2/dof . Interestingly, the pole and dispersive parameterizations result in very similar values for $\ln C$, while the quadratic and z -parameterization results are similar. This can in fact be easily understood from the Appendix which presents a detailed investigation of the correlations between parameters in the different parameterizations. All of the $\ln C$ results are consistent within $2\sigma_{stat}$, as can be deduced from the difference of the χ^2 (4 units per one degree of freedom change) and by estimating the uncertainty of the difference as a difference of the uncertainties in quadrature: $\ln C|_{disp/disp} - \ln C|_{z/disp} = 0.026 \pm 0.013$.

A similar level of agreement between the different parameterizations is observed for the I_K integrals. For example for $K_{L\mu 3}$ data, using the z -parameterization with two parameters for each of the vector and scalar form factors, one obtains $I_K^e|_z = 0.15331 \pm 0.00072_{stat} \pm 0.00040_{syst}$ and $I_K^\mu|_{z/z} = 0.10101 \pm 0.00053_{stat} \pm 0.00039_{syst}$.

IV. DISCUSSION

While both the z and dispersive parameterizations give rigorous bounds on theoretical uncertainties, the latter uses additional experimental input such as the low energy $K\pi$ phase shifts. This allows for a one-parameter fit of the vector and scalar form factors, resulting in smaller uncertainties. In the following, we discuss the impact of the value obtained for $\ln C$, in the dispersive parameterization.

A. Comparison with lattice results

Here we compare our result for $\ln C$ against the lattice QCD calculations. This comparison does not depend on SM assumptions since no electroweak couplings are involved.

Figure 1 shows lattice QCD results for F_K/F_π and $f_+(0)$ in the 2+1 flavor case [18, 19, 20, 21, 22, 23]. A first classification of these data can be found in the recent proceeding Ref. [24] awaiting for the FLAVIANet Lattice Averaging Group’s one. We have only considered published results and showed them as bands including systematic and statistical errors not giving the central values for clarity. Note that RBC/UKQCD has much bigger systematic errors compared to the other collaborations leading to the rather large band for F_K/F_π ranging from 1.14 to 1.27.

Also shown is the $f_+(0)$ vs F_K/F_π dependence as derived from Eq. (3) using our result for $\ln C$ [42]. For Δ_{CT} ,

	Parameterization Vector FF/Scalar FF			
Results	disp.(I)/disp.	pole(I)/disp.	quad (II)/disp.	z-param.(II)/disp.
Fit param. v_i	$\Lambda_+ = 24.57(83)$	$M_V = 890.00$ (13.00)MeV	$\lambda'_+ = 17.5(3.4)$ $\lambda''_+ = 4.3(1.4)$	$a_1 = 1.057(63)$ $a_2 = 3.9(3.2)$
λ'_+	24.57(83)	24.59(72)	17.5(3.4)	20.00(2.60)
λ''_+	1.19(4)	1.21(7)	4.3(1.4)	2.5(6)
Fit param. $\ln C$	0.1947(91)	0.1944(93)	0.169(16)	0.170(16)
λ_0	13.22(78)	13.20(79)	11.03(1.37)	11.11(1.37)
λ'_0	0.59(2)	0.59(2)	0.54(3)	0.54(3)
$\rho(v_i, \ln C)$	-0.557	0.588	0.707	0.477
	-	-	-0.819	-0.766
χ^2/dof	193/236	193/236	189/235	189/235

TABLE II: Results of the fit to $K_{L\mu 3}$ data using different parameterizations for the vector form factor and the dispersive one for the scalar form factor. The uncertainties are only statistical. Λ_+ , λ'_+ , λ''_+ , λ_0 and λ'_0 are in units 10^3 .

	Parameterization Vector FF			
Results	dispersive (I)	pole (I)	quadratic (II)	z-param. (II)
Fit param.	$\Lambda_+ = 25.17(38)$	$M_V = 881.03$ (5.91)MeV	$\lambda'_+ = 21.67(1.59)$ $\lambda''_+ = 2.87(66)$	$a_1 = 1.023(28)$ $a_2 = 0.75(1.58)$
λ'_+	25.17(38)	25.10(41)	21.67(1.59)	22.69(1.20)
λ''_+	1.22(4)	1.26(3)	2.87(66)	1.93(30)
Correlation	-	-	-0.96	-0.064
χ^2/dof	66.6/65	66.3/65	62.2/64	62.3/64

TABLE III: Results of the fit to K_{Le3} data using different parameterizations with only the statistical uncertainties. Pole, quadratic and z-parameterization results are from Refs. [1] and [10]. Λ_+ , λ'_+ and λ''_+ are in units 10^3 .

we have used the value [25]

$$\Delta_{CT} = -0.0035 \pm 0.0080, \quad (12)$$

taken from a next-to-leading-order calculation in chiral perturbation theory in the isospin limit. The error is a conservative estimate of higher order corrections in the quark masses m_u , m_d and m_s [26]. This value of Δ_{CT} is in agreement with other recent determinations [27, 28, 29, 30].

Combining all the lattice results, the grey band in the $f_+(0)$ vs F_K/F_π plane shown in Fig. 1, is obtained. Comparing this band to the KTeV result, the ranges $F_K/F_\pi < 1.20$ and $f_+(0) > 0.96$ are favoured by the KTeV data.

B. Test of the SM

As mentioned in § I, the small size of the Δ_{CT} correction allows for an accurate SM test using the Callan

Treiman relation, now rewritten as

$$\frac{F_K}{F_\pi \cdot f_+(0)} = C - \Delta_{CT}. \quad (13)$$

This test consists of comparing the value of $F_K/(F_\pi \cdot f_+(0))$, deduced from the $K_{L\ell 3}$ dispersive form factor parametrization fit, to the value of $F_K/(F_\pi \cdot f_+(0))|_{SM}$, determined by assuming the SM electroweak (EW) couplings and using the experimental (photon inclusive) branching fractions $\Gamma_{K_{\mu\nu}^+}/\Gamma_{\pi_{\mu\nu}^+}$ and $\Gamma_{K_{Le3}}$ measurements.

We define r as

$$r = (C - \Delta_{CT}) \cdot \left(\frac{F_\pi \cdot f_+(0)}{F_K} \right) \Big|_{SM}. \quad (14)$$

Physics beyond the SM, such as modifications of EW couplings of quarks due to new exchanges close to the TeV scale, could cause r to differ from unity. An example of modified EW couplings between right-handed quarks and the W boson is discussed in Refs. [2, 31].

We first calculate $F_K/(F_\pi \cdot f_+(0))|_{SM}$. Assuming the

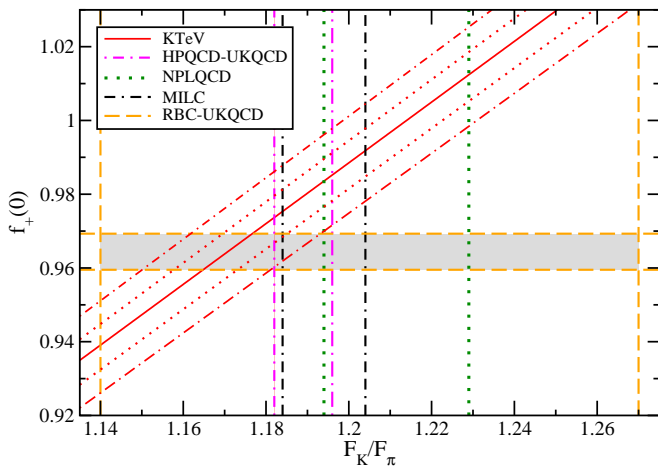


FIG. 1: The constraints on $f_+(0)$ and F_K/F_π from various lattice QCD calculations. The KTeV result for $F_K/(F_\pi \cdot f_+(0))$ is shown as the red solid line, derived by using the Callan Treiman relation and the NLO result for Δ_{CT} . Also shown is the error due to Δ_{CT} (red dotted lines), and the resulting error when added in quadrature to the total error on C as given in Eq. (8) (red dot-dashed line).

SM couplings, one has

$$\begin{aligned} & \frac{\Gamma[K \rightarrow l\nu_l(\gamma)]}{\Gamma[\pi \rightarrow l\nu_l(\gamma)]}|_{SM} \\ &= \text{cte} \frac{|V_{us}|^2}{|V_{ud}|^2} \frac{F_K^2 m_K}{F_\pi^2 m_\pi} \frac{(1-x_K^2)^2}{(1-x_\pi^2)^2} \frac{[1 + \frac{\alpha}{\pi} F(x_K)]}{[1 + \frac{\alpha}{\pi} F(x_\pi)]} \\ &= \mathcal{M}^2 \left(\frac{F_K V_{us}}{F_\pi V_{ud}} \right)^2, \end{aligned} \quad (15)$$

where $x_P \equiv m_l/M_P$. The expression for cte, which depends on the hadronic structure and particle masses, can be found in Ref. [35]. The function $F(x)$ parametrizes the electromagnetic radiative corrections, and α is the fine structure constant. The coefficient \mathcal{M} thus defined is equal to 0.2387(4) (see Ref. [36]).

The K_{Le3} partial width is expressed as

$$\Gamma_{K_{Le3}}|_{SM} = \mathcal{N}^2 |f_+(0)V_{us}|^2, \quad (16)$$

where

$$\mathcal{N}^2 = G_F^2 \frac{m_K^5}{(192\pi^3)} S_{EW} (1 + \delta_K^e) I_K^e. \quad (17)$$

Here G_F is the Fermi constant, S_{EW} are short-distance electroweak corrections, and δ_K^e denotes the electromagnetic (EM) radiative corrections. From equations (15) and (16), it can be shown that

$$\frac{F_K}{F_\pi \cdot f_+(0)}|_{SM} = \left(\frac{\Gamma_{K_{\mu\nu}^+}}{\Gamma_{\pi_{\mu\nu}^+} \cdot \Gamma_{K_{Le3}}} \right)^{1/2} \cdot |V_{ud}| \cdot \frac{\mathcal{N}}{\mathcal{M}}. \quad (18)$$

Using the world average result [36] $\Gamma_{K_{\mu\nu}^+}/\Gamma_{\pi_{\mu\nu}^+} = 1.3337(46)$, the KTeV measurement of $\Gamma_{K_{Le3}} =$

0.4067(11) [1], the values of I_K^e from Table I and $\delta_K^e = 0.0130(30)$ from Ref. [39], and the value of $|V_{ud}|$ inferred from $0^+ \rightarrow 0^+$ superallowed nuclear transitions [37][43],

$$|V_{ud}| = 0.97418(26), \quad (19)$$

Eq. (18) gives the result

$$\frac{F_K}{F_\pi \cdot f_+(0)}|_{SM} = 1.2407 \pm 0.0044. \quad (20)$$

This result can be compared with the experimental determination of $F_K/(F_\pi \cdot f_+(0))$ through $K_{L\ell 3}$ decay as given in Table 1. One obtains

$$r = 1.0216 \pm 0.0124_{\text{exp}} \pm 0.0039_{\text{theo}} \pm 0.0067_{\Delta_{CT}}. \quad (21)$$

The first two errors come from the experimental and the theoretical uncertainties on $\ln C$ respectively, and the last error comes from the estimated error on Δ_{CT} [44]. Adding the different errors in quadrature, we obtain $r = 1.0216 \pm 0.0146$.

Analogous to Fig. 1, Fig. 2 shows the two bands in the $f_+(0)$ -vs- F_K/F_π plane. The first band (red) shows the dispersive parametrization analysis of the KTeV $K_{L\ell 3}$ data. The second band (green) shows the SM prediction, Eq. (20). We observe a 1.5σ difference between the KTeV result and the SM prediction.

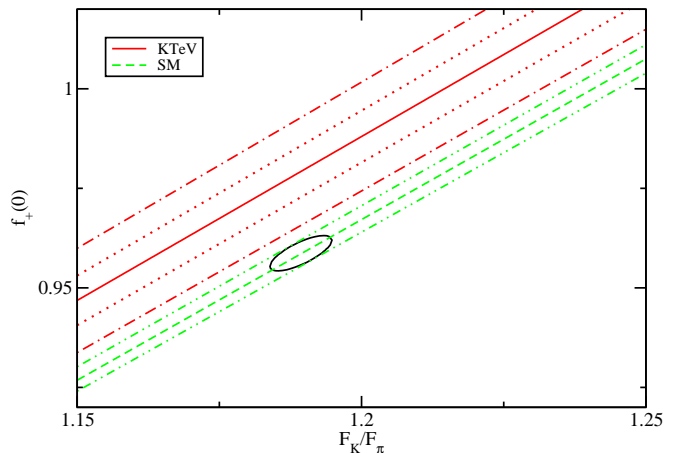


FIG. 2: The constraints on $f_+(0)$ and F_K/F_π . The inserted $\chi^2 - \chi_{MIN}^2 = 1$ ellipse is the SM result obtained from Eqs. (15) and (16) and the CKM unitarity. The dashed green line and its error bar (green dotted line) corresponds to $F_K/(F_\pi \cdot f_+(0))|_{SM}$, calculated using the measured decay widths and assuming the SM couplings of light quarks, Eq. (20). Shown in red is the $F_K/(F_\pi \cdot f_+(0))$ result, derived from the dispersive parameterization fit to KTeV data and the NLO result for Δ_{CT} . Also shown is the error due to Δ_{CT} (red dotted lines) added in quadrature to the total error on C as given in Eq. (8) (red dot-dashed line).

Separate bounds on $F_K/F_\pi|_{SM}$ and $f_+(0)|_{SM}$ can be derived from CKM unitarity [31, 40]. Unitarity implies

that $|V_{ud}|^2 + |V_{us}|^2 + |V_{ub}|^2 = 1$, and measurements involving $b \rightarrow u$ transitions have shown that $|V_{ub}|^2$ is negligibly small. Consequently, the SM mixing of light quarks is entirely specified by the value of $|V_{ud}|$.

Substituting $|V_{us}|^2 = 1 - |V_{ud}|^2$ into equations (15) and (16), and solving for F_K/F_π and $f_+(0)$, we obtain the contour in Fig. 2. One has

$$\begin{aligned} F_K/F_\pi|_{SM} &= 1.189 \pm 0.007 \\ f_+(0)|_{SM} &= 0.959 \pm 0.006. \end{aligned} \quad (22)$$

With the current experimental precision, the data show a marginal agreement with the SM as concluded before.

C. Ratio G_F^μ/G_F^e

Taking the ratio of the K_{Le3} to $K_{L\mu3}$ partial widths, without assuming the equality of the $G_F^{\mu,e}$ decay constants, one obtains

$$\left(\frac{G_F^\mu}{G_F^e}\right)^2 = \left[\frac{\Gamma(K_L \rightarrow \pi^\pm \mu^\mp \nu)}{\Gamma(K_L \rightarrow \pi^\pm e^\mp \nu)}\right] / \left(\frac{1 + \delta_K^\mu}{1 + \delta_K^e} \cdot \frac{I_K^\mu}{I_K^e}\right). \quad (23)$$

Using the value of I_K^μ/I_K^e from Table 1, the EM correction estimates $(1 + \delta_K^\mu)/(1 + \delta_K^e) = 1.0058 \pm 0.0010$ from Ref. [39],[45] and the direct measurement of $\Gamma(K_L \rightarrow \pi^\pm \mu^\mp \nu)/\Gamma(K_L \rightarrow \pi^\pm e^\mp \nu) = 0.6640 \pm 0.0014 \pm 0.0022$ from Ref. [1], one obtains

$$\mathcal{R}_{\mu/e} \equiv \left(\frac{G_F^\mu}{G_F^e}\right)^2 = 0.9978 \pm 0.0049. \quad (24)$$

This result is in excellent agreement with the Standard Model expectation of unity, and it is very similar to the previous KTeV result, $(G_F^\mu/G_F^e)^2 = 0.9969 \pm 0.0048$. Although the I_K^μ and I_K^e phase-space uncertainties in Table I are smaller than in the previous KTeV analysis [1], the uncertainty on $\mathcal{R}_{\mu/e}$ is almost identical in these two analyses. This is due to the fact that the uncertainties on the radiative corrections dominate the uncertainties on this ratio. In both analyses, the uncertainty on the ratio of phase-space integrals, I_K^μ/I_K^e , is significantly smaller than the quadrature-sum of the individual uncertainties because of correlations in the vector form factor (f_+). In the KTeV analysis, the theoretical uncertainty related to the scalar form factor (f_0) could not be evaluated because of the parameterization used. In this analysis using the dispersive parameterization, the f_0 uncertainty is more reliable, resulting in a more robust estimate of the uncertainty on $\mathcal{R}_{\mu/e}$.

V. SUMMARY

A dispersive analysis of the semileptonic form factors for K_{Le3} and $K_{L\mu3}$ has been performed based on the published KTeV data.

The measured value of $\ln C$, the scalar form factor at the Callan-Treiman point, leads to a dependence of $f_+(0)$ on F_K/F_π within 1.5σ of the Standard Model prediction. It favors an F_K/F_π value on the lower side of the lattice results, and an $f_+(0)$ value on the higher side. New values of the decay phase space integrals I_K^μ and I_K^e are obtained, where the latter is consistent with the result obtained by z parametrization [10]. These new values can be used to determine the ratio of the decay constants of the two semileptonic modes, G_F^μ/G_F^e , which is in excellent agreement with the Standard Model prediction. A detailed analysis of a Taylor-expansion vector form factor fit to the data is used to study how the scalar and vector form factor correlations affect the result for $\ln C$.

APPENDIX A: PARAMETER CORRELATIONS

In this Appendix, we will investigate correlations between parameters in the different form factor parameterizations. This study helps to understand several results discussed in the text, especially the difference between the parameterizations used for the vector form factor presented in Sec. III, and the robustness of the dispersive result presented in Sec. II.

For this study, we will perform several fits of the $K_{L\mu3}$ data. We will always use the dispersive parameterization for the scalar form factor. For the vector form factor, we will consider a cubic expansion, i.e., the first three terms of Eq. (1) will be taken into account. Indeed, in the physical region of $K_{L\mu3}$ decay, a good representation of the dispersive parameterization may be obtained by Taylor expanding it with respect to t and keeping only the first three terms. We thus have four parameters ($\ln C$, λ'_+ , λ''_+ , and λ'''_+) which will enter the fitting procedure.

Let us first fix the third order coefficient λ'''_+ to zero, which corresponds to a fit with a quadratic parameterization for the vector form factor. We then perform a fit with two free parameters, namely $\ln C$ and λ'_+ , while fixing the curvature λ''_+ to three different values: $\lambda''_+ = 0.001, 0.002$ and 0.003 ($\lambda''_+ = 0.0$ would correspond to a linear parameterization for the vector form factor, which gives a very poor fit to the data). The results of these fits are shown by the black points on Fig. 3. The value of λ'_+ can be read on the y axis and $\ln C$ is given by the first number in parentheses above each black point; the second number in parentheses gives the χ^2 of the fit. The linear relationship between λ'_+ and λ''_+ seen on the figure shows the strong correlation between these two quantities. For example, a fit to K_{e3} data using a quadratic parameterization for the vector form factor leads to a correlation, $\rho(\lambda'_+, \lambda''_+) = -0.96$ [1]. A similar linear dependence is also obtained between $\ln C$ and λ'_+ or λ''_+ . Furthermore, when moving toward larger λ''_+ , $\ln C$ decreases while the χ^2 decreases only slightly. The green square at the end of the solid black line represents the minimum χ^2 ; it corresponds to the result of the quadratic/dispersive fit given in Section III. (We have stopped the line at that value

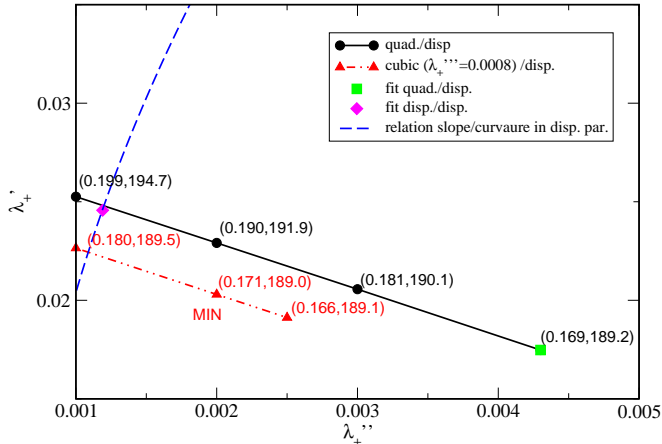


FIG. 3: Dependence of the fitted values of $\ln C$ and λ'_+ on the curvature, λ''_+ . The value of $\ln C$ and the χ^2 of the corresponding fit are given in parenthesis above each point. To simulate the presence of higher order terms in the z -parameterization, for the red line a third order term has been included. The effect of this third order term is only to shift the curve downwards. In the legend, "quad./disp." for example indicates that a "quadratic" parametrization is used for the vector form factor and a "dispersive" one for the scalar.

of the curvature for convenience.)

Next, we consider the impact of a third-order term in the Taylor expansion. Indeed, a dispersive or z -parameterization of the vector form factor gives a nonzero value for the third order coefficient λ''_+ when Taylor expanded. We repeat the same procedure as above (i.e., floating $\ln C$ and λ'_+ , and varying λ''_+), but the third-order coefficient is now fixed to $\lambda''_+ = 0.0008$, close to what is obtained from the results of the z -parameterization (Tables II and III). The nonzero λ''_+ causes an offset in the linear dependence of λ'_+ with λ''_+ , but leads to the same slope and a similar variation of $\ln C$ with the slope and the curvature (see the red dot-dot-dashed line on Fig. 3) [46]. The minimum χ^2 fit (green square for $\lambda''_+ = 0$) is now moved toward a smaller λ'_+ and a larger λ''_+ (red triangle denoted by 'MIN'). This point corresponds to the z -parameterization result in Table II.)

The parameter shifts are required in order to compensate for the additional cubic term. Note that the value of $\ln C$ is roughly the same at this minimum as the one obtained previously for $\lambda''_+ = 0$.

In the light of this study, let us now consider the other parameterizations used in the literature [1], [10], [16], [15]. One can distinguish two classes. One class (Class I), of which the dispersive and pole parameterizations are examples, impose physically motivated relations between the slope and the curvature (and possibly the higher order terms in the Taylor expansion, the third order term being the most relevant one in the physical region). Indeed, as already emphasized, in the dispersive parameterization the curvature and all higher order terms of the vector form factor are constrained not only on first principles, such as analyticity and unitarity, but also by including the information on the low energy $K\pi P$ -waves (K^* resonance). The relation between slope and curvature is illustrated by the blue dashed curve in Fig. 3. This curve crosses the black solid line and the red dot-dot-dashed line for large values of λ'_+ , small values of λ''_+ , and consequently large values for $\ln C$, nicely illustrating the result of the dispersive/dispersive fit (magenta diamond in the figure). In contrast, the second class (Class II), of which the Taylor series and z -parameterization are examples, is based on mathematically rigorous expansions, in which the slope and curvature are free parameters. Clearly, the existence of a relation between slope and curvature strongly constrains the fit in Class I, while the fit has more freedom when using Class II parameterizations. One thus expects smaller fitting uncertainties in the results from the Class I and larger ones from Class II, so that if the theoretical errors are well controlled, the overall uncertainty will be smaller for class I.

Acknowledgments

One of us (V. B.) would like to thank S. Descotes-Genon and B. Moussallam for interesting discussions. This work has been partially supported by the EU contract MRTN-CT-2006-035482 ("Flavianet"), the EU Integrated Infrastructure Initiative Hadron Physics (RH3-CT-2004-506078), the Swiss National Science Foundation and the IN2P3 projet th orie "Signature exp rimentale des couplages  lectrofaibles non-standards des quarks".

-
- [1] T. Alexopoulos *et al.* [KTeV Collaboration], Phys. Rev. Lett. **93** (2004) 181802 [arXiv:hep-ex/0406001]; Phys. Rev. D **93** (2004) 092006 [arXiv:hep-ex/0406002]; Phys. Rev. D **70** (2004) 092007 [arXiv:hep-ex/0406003].
 - [2] V. Bernard, M. Oertel, E. Passemar and J. Stern, Phys. Lett. B **638** (2006) 480 [arXiv:hep-ph/0603202].
 - [3] V. Bernard, M. Oertel, E. Passemar and J. Stern, Phys. Rev. D **80** (2009) 034034 [arXiv:0903.1654 [hep-ph]].
 - [4] P. Franzini, Kaon International Conference (KAON 2007), PoS(KAON)002 (2007).
 - [5] A. Lai *et al.* [NA48 Collaboration], Phys. Lett. B **602** (2004) 41 [arXiv:hep-ex/0410059].
 - [6] O. P. Yushchenko *et al.*, Phys. Lett. B **589** (2004) 111 [arXiv:hep-ex/0404030]; Phys. Lett. B **581** (2004) 31 [arXiv:hep-ex/0312004].
 - [7] F. Ambrosino *et al.* [KLOE Collaboration], Phys. Lett. B **632** (2006) 43 [arXiv:hep-ex/0508027].
 - [8] T. Becher and R. J. Hill, Phys. Lett. B **633**, 61 (2006) [arXiv:hep-ph/0509090].
 - [9] R. J. Hill, Phys. Rev. D **74**, 096006 (2006)

- [arXiv:hep-ph/0607108].
- [10] E. Abouzaid *et al.* [KTeV Collaboration], Phys. Rev. D **74**, 097101 (2006) [arXiv:hep-ex/0608058].
- [11] P. Buettiker, S. Descotes-Genon and B. Moussallam, Eur. Phys. J. C **33** (2004) 409 [arXiv:hep-ph/0310283].
- [12] P. Estabrooks *et al.*, Nucl. Phys. B **133** (1978) 490.
- [13] D. Aston *et al.*, Nucl. Phys. B **296** (1988) 493.
- [14] R. F. Dashen and M. Weinstein, Phys. Rev. Lett. **22**, 1337 (1969).
- [15] A. Lai *et al.* [NA48 Collaboration], Phys. Lett. B **647** (2007) 341 [arXiv:hep-ex/0703002].
- [16] F. Ambrosino *et al.* [KLOE Collaboration], JHEP **0712** (2007) 105 [arXiv:0710.4470 [hep-ex]].
- [17] K. M. Watson, Phys. Rev. **88** (1952) 1163.
- [18] C. Aubin *et al.* [MILC Collaboration], Phys. Rev. D **70** (2004) 114501 [arXiv:hep-lat/0407028]; C. Bernard *et al.* [MILC Collaboration], PoS **LAT2006** (2006) 163 [arXiv:hep-lat/0609053]; C. Bernard *et al.*, PoS **LAT-TICE2007** (2006) 090 [arXiv:0710.1118 [hep-lat]].
- [19] E. Follana, C. T. H. Davies, G. P. Lepage and J. Shigemitsu [HPQCD Collaboration], Phys. Rev. Lett. **100** (2008) 062002 [arXiv:0706.1726 [hep-lat]].
- [20] S. R. Beane, P. F. Bedaque, K. Orginos and M. J. Savage, Phys. Rev. D **75** (2007) 094501 [arXiv:hep-lat/0606023].
- [21] C. Allton *et al.* [RBC and UKQCD Collaborations], Phys. Rev. D **76** (2007) 014504 [arXiv:hep-lat/0701013].
- [22] C. Allton *et al.* [RBC-UKQCD Collaboration], Phys. Rev. D **78** (2008) 114509 [arXiv:0804.0473 [hep-lat]].
- [23] P. A. Boyle *et al.*, Phys. Rev. Lett. **100** (2008) 141601 [arXiv:0710.5136 [hep-lat]].
- [24] L. Lellouch, arXiv:0902.4545 [hep-lat].
- [25] J. Gasser and H. Leutwyler, Nucl. Phys. B **250** (1985) 517.
- [26] H. Leutwyler, private communication.
- [27] M. Jamin, J. A. Oller and A. Pich, JHEP **0402** (2004) 047 [arXiv:hep-ph/0401080].
- [28] J. Bijnens and K. Ghorbani, arXiv:0711.0148 [hep-ph].
- [29] V. Bernard, E. Passemar, Phys. Lett. B **661**, 95 (2008) [arXiv:0711.3450 [hep-ph]].
- [30] A. Kastner and H. Neufeld, Eur. Phys. J. C **57** (2008) 541 [arXiv:0805.2222 [hep-ph]].
- [31] V. Bernard, M. Oertel, E. Passemar and J. Stern, JHEP **0801** (2008) 015 [arXiv:0707.4194 [hep-ph]].
- [32] Flavianet Working Group on Kaon Decays, M. Antonelli *et al.*, Nucl. Phys. Proc. Suppl. **181-182** (2008) 83 [arXiv:0801.1817 [hep-ph]].
- [33] G. Furlan, F. G. Lannoy, G. Rossetti and G. Segre, Nuovo Cim, **38** (1965) 1747.
- [34] J. Stern, private communication.
- [35] W.J. Marciano and A. Sirlin, Phys. Rev. Lett. **71** (1993) 3629.
- [36] E. Blucher and W. J. Marciano, in C. Amsler *et al.* [Particle Data Group], Physics Letters **B667** (2008) 1.
- [37] I. S. Towner and J. C. Hardy, Phys. Rev. C **77** (2008) 025501 [arXiv:0710.3181 [nucl-th]].
- [38] J. C. Hardy and I. S. Towner, arXiv:0812.1202 [nucl-ex].
- [39] T. C. Andre, Annals Phys. **322** (2007) 2518 [arXiv:hep-ph/0406006].
- [40] J. Stern, Nucl. Phys. Proc. Suppl. **174** (2007) 109 [arXiv:hep-ph/0611127].
- [41] V. Cirigliano, M. Knecht, H. Neufeld, H. Rupertsberger and P. Talavera, Eur. Phys. J. C **23** (2002) 121 [arXiv:hep-ph/0110153]; V. Cirigliano, H. Neufeld and H. Pichl, Eur. Phys. J. C **35** (2004) 53 [arXiv:hep-ph/0401173]; V. Cirigliano, M. Giannotti and H. Neufeld, JHEP **0811** (2008) 006 [arXiv:0807.4507 [hep-ph]].
- [42] Note that we have plotted $f_+(0)$ up to 1.02, though the Fubini Furlan bound [33] claims $f_+(0) \leq 1$. However, in QCD this bound can only be proven in the large N_c limit, leaving the possibility for a slight deviation from it [34].
- [43] Note that a recent update [38] has appeared.
- [44] Note that this analysis of the KTeV data holds if there are no scalar, pseudoscalar and tensor couplings. Indeed in the presence of the two former what has been measured in table 1 is not $\ln C$ but $\ln C$ plus a small quantity, see Ref. [32]. Consequently in that case a determination of r is not possible without a precise knowledge of these couplings.
- [45] To maintain consistency of this analysis with that of [1], the EM correction ratio has been taken from Ref. [39]. Recently, new radiative correction estimates have appeared based on ChPT calculations [41], which are in agreement with the old results but with a larger uncertainty.
- [46] Note that for illustration purpose we only show a portion of this line as well as of the black solid line corresponding to the fits we have made. They of course go on in both directions.